Acta Biomaterialia xxx (xxxx) xxx

Contents lists available at ScienceDirect

Acta Biomaterialia

journal homepage: www.elsevier.com/locate/actbio

Full length article

A prevascularized nerve conduit based on a stem cell sheet effectively promotes the repair of transected spinal cord injury

Zengjie Fan[a,*], Xiaozhu Liao[a], Yu Tian[a], Xie xuzhuzi[a], Yingying Nie[b,*]

[a] School of Stomatology, Lanzhou University, Lanzhou 730000, PR China
[b] Institute of Sensing Technology, Gansu Academy of Sciences, Lanzhou 730000, PR China

ARTICLE INFO

Article history:
Received 2 November 2018
Revised 15 October 2019
Accepted 29 October 2019
Available online xxx

Keywords:
Stem cell
Prevascularization
Cell sheet
Spinal cord injury

ABSTRACT

Spinal cord injury (SCI) can result in severe loss of motor and sensory function caused by ischemia and hypoxia, which are the key limiting factors of SCI rehabilitation. Vascularization is considered an effective way to resolve the issues of ischemia and hypoxia. In this regard, we first fabricated prevascularized nerve conduits (PNC) based on the prevascularized stem cell sheet and evaluated their repair effects by implanting them into transected SCI rats. A better healing effect was presented in the PNC group than in the control group and the nonprevascularized nerve conduit (NPNC) group as shown in H&E staining and the Basso, Beattie, Bresnahan (BBB) Locomotor Rating Scale assessment. In addition, the expression of β-III tubulin (Tuj-1) in the PNC group was higher than that in the control group and the NPNC group because of the introduction of MSCs. Conversely, the expression of the glial fibrillary acidic protein (GFAP) in both experimental groups was lower than that in the control group because of the inhibitory effect of MSCs on glial scar formation. Taken together, the introduction of prevascularization into the neuron conduit was an effective solution for improving the condition of ischemia and hypoxia, inhibiting glial scar formation, and promoting the healing of SCI, which implied that the PNC may be a potential alternative material to biomaterials for SCI rehabilitation.

Statement of significance

1. Prevascularized stem cell sheet was first used to repair spinal cord injury (SCI).
2. Prevascularized stem cell sheet use can effectively resolve the challenges faced during SCI, including ischemia and hypoxia and the limited regenerative ability of the remained neurons.
3. Prevascularized stem cell sheet was found to accelerate the healing of SCI as compared to those in the control group and the pure stem cell sheet group.
4. The introduction of stem cells can effectively inhibit the formation of a glial scar.

© 2019 Acta Materialia Inc. Published by Elsevier Ltd. All rights reserved.

1. Introduction

Spinal cord injury (SCI) is a devastating injury to the structure and function of the spinal neuron, resulting in the loss of motor and sensory function below the damaged point, which causes patients to suffer huge economic loss burden and endless pain [1,2]. SCI can be divided into two stages: primary and secondary injury [3]. After mechanical trauma, the destruction of the spinal cord and its surrounding vascular tissues leads to local edema, ischemia, and hypoxia, which are the causes of primary injury [4]. The main inducements to secondary injury are ischemia and hypoxia derived from the primary injury, causing infiltration of inflammatory cells and apoptosis and necrosis of neurons [5]. Thus, ischemia and hypoxia have the potential to worsen the pathological process and delay the recovery of SCI. In addition, the limited regenerative ability of the remained neurons is the second reason for the delayed healing of SCI [6].

To resolve the issues of ischemia and hypoxia, the present methods focus on the angiogenesis around the SCI sites, including the application of vascular endothelial growth factor (VEGF) and angiopoietin-1 [7–9], the addition of endothelial progenitor cells

* Corresponding authors.
E-mail addresses: zjfan@lzu.edu.cn (Z. Fan), yingyingnie@126.com (Y. Nie).

https://doi.org/10.1016/j.actbio.2019.10.042
1742-7061/© 2019 Acta Materialia Inc. Published by Elsevier Ltd. All rights reserved.

Please cite this article as: Z. Fan, X. Liao and Y. Tian et al., A prevascularized nerve conduit based on a stem cell sheet effectively promotes the repair of transected spinal cord injury, Acta Biomaterialia, https://doi.org/10.1016/j.actbio.2019.10.042

[10], and the application of vascularized nerve flap [11], where agreement can be reached that vascularization effectively promotes SCI recovery. However, it is difficult to effectively control the release of growth factors in the spatiotemporal dimensions. For endothelial progenitor cells, only limited vascularization can be produced because of the application of the single cell source. Another injury can result from vascularized nerve flap obtained from patients' tissues.

To overcome the second issue, that is, the limited regenerative ability of the remained neurons around the damaged area, various stem cell sources have been used for SCI repair, including mesenchymal stromal cells (MSCs) [12], neural stem cells [13], embryonic stem cells [14], and induced pluripotent stem cells [15]. MSCs can be easily isolated and cultured with high potential for multilineage differentiation. More importantly, MSCs have minimal or no immunoreactivity and graft-versus-host reaction of transplanted allogeneic MSCs [16]. Presently, MSC injections and MSC seeding in scaffold materials are the two commonly used methods with the drawbacks of low seeding density, cell loss, and immunogenicity of the scaffold materials, which limit their application in SCI repair [17–19].

An innovative technology, termed cell sheet technology (CST), is used to fabricate the cell sheet. An intact and contiguous cell sheet, composed of cells and extracellular matrix (ECM), can be obtained without enzymatic digestion, and this enables cell bioactivity to be kept completely and the adverse impact of biomaterials to be avoided effectively [20]. Additionally, the cell sheet has a high adhesive ability depending on fibronectin, which can be transplanted or grafted to the host tissues without using any suture [21]. Therefore, cell sheet is widely applied in the repair of various tissues including the skin, liver, heart, cornea, and periodontal tissues [21–25]. Unfortunately, only few studies have reported its application in neuron repair. Hence, it is highly urgent and necessary to explore the repair potency of stem cell sheet for SCI.

By employing CST, a prevascularized cell sheet can be fabricated by co-culturing two different kinds of cells, namely, MSCs and endothelial cells (ECs), to facilitate the formation of microvascular networks on the cell sheet [26]. Prevascularization plays an important role in maintaining the survival of the transplanted tissues as well as in accelerating the repair of the defect area by supplying sufficient nutrition and oxygen. As reported, ischemia and hypoxia are the main causes of the primary and secondary injury of SCI. If a prevascularized cell sheet is used to repair the SCI, then these causes may be addressed effectively. We previously fabricated a prevascularized cell sheet by co-culturing MSCs and ECs and found that the differentiation potency of MSCs can be effectively kept [27], which could provide hope to improve the poor regenerative ability of the remained neurons around the damaged area.

Herein, to resolve the two key issues of SCI recovery, namely, ischemia and hypoxia and the limited regeneration ability, first, we originally prepared prevascularized nerve conduits (PNC) based on the stem cell sheet and then the fabricated nerve conduits (NC) were implanted into the transected SCI of SD rats to assess the healing effect during 8 weeks of experiment. The locomotor behaviors were assessed by the BBB method. The healing effect was quantified through histochemistry and immunohistochemistry with an aim to provide a new repair solution for SCI and expand the range of cell sheet application in clinic.

2. Material and method

2.1. Rabbit MSC isolation and culture

Chinese big-ear white rabbits aged 2 weeks and weighing 180 to 200 g were provided by the Lanzhou Veterinary Research Institute of the Chinese Academy of Agricultural Sciences without sex limitation. All experiments were performed under the guideline of caring laboratory animals of the Ministry of Science and Technology of the People's Republic of China.

The rabbits were anesthetized and soaked entirely in 75% alcohol for 20 min. The tibia and femur were isolated on an aseptic table and then quickly soaked in PBS buffer. After removing the soft tissues attached to the tibia and femur on a super-clean worktable, both ends of the tibia and femur were cut with an aseptic scissors. Next, the bone marrow was flushed out 4–5 times using a 5 mL syringe containing DMEM. The obtained bone marrow solution was centrifuged (1200 rpm) for 5 min. Accomplishing this, the sediment was resuspended in 8 mL DMEM/F12 medium after removing the supernatant, and then sub-packed in aseptic 25 cm^2 culture flasks. Further, the flasks were incubated at 37 °C in humidified air containing 5% CO_2. Twenty-four hours later, the flasks were gently shaken to suspend the unattached cells. Four milliliters of DMEM/F12 medium was used to refresh the culture medium. Subsequently, the culture medium was changed every 48 h to further purify the cells. The growth status of cells was recorded using an inverted optical microscope. When the confluence of the cell clones reached more than 80%, the cells were passaged and cultured. The induced differentiation of BMSCs was also conducted, including osteoblastic, adipogenic, and neurogenic differentiation, to identify the multipotency of the MSCs. In addition, the stemness of the obtained BMSCs was identified by immunofluorescence staining, including CD 29, CD 44, and CD 90.

2.2. MSC cell sheet preparation

MSCs were seeded into 6-well plates at a density of 9×10^4 cells/cm^2 and cultured in DMEM complete medium. To accelerate the secretion of ECM and promote cell sheet formation, 30 mM glucose and 50 μg/mL ascorbic acid were added to the DMEM complete medium. The medium was changed every two days, and the cells were cultured for 14 days to obtain a dense and contiguous cell sheet.

2.3. Prevascularized MSC cell sheet preparation

After 14 days, human umbilical vein endothelial cells (HUVECs) were seeded onto the surface of the MSC cell sheet at a density of 5×10^4 cells/cm^2 and cultured for another 7 days. The culture medium was refreshed every two days.

2.4. Nerve conduit based on MSC cell sheet and prevascularized MSC cell sheet

After incubating for 14 days in the 100 × 100 mm culture dish, the obtained MSC cell sheet and prevascularized MSC cell sheet were cut into several strips with a width of 20 mm and rolled layer by layer into nonprevascularized nerve conduits (NPNC) and PNC by using PTFE tube (diameter = 1.6 mm) as a model, respectively. When the conduits were cultured in different culture media for another 7 days, the cell sheets fused with each other and the thickness of the conduit was reduced. The NC could stand on a flat surface independently when the PTFE tube was removed, indicating it was successfully prepared.

2.5. SEM sample preparation

The obtained NPNC and PNC were fixed in 4% paraformaldehyde solution for 24 h, washed with PBS three times, and dehydrated using graded ethanol, followed by drying at room temperature and coating with gold for SEM observation (SEM, JEOL JSM-6701F).

Please cite this article as: Z. Fan, X. Liao and Y. Tian et al., A prevascularized nerve conduit based on a stem cell sheet effectively promotes the repair of transected spinal cord injury, Acta Biomaterialia, https://doi.org/10.1016/j.actbio.2019.10.042

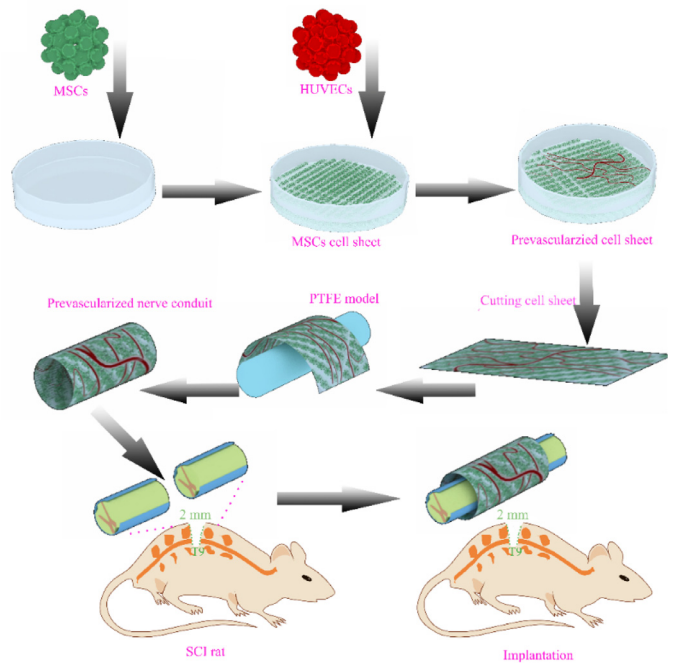

Fig. 1. Schematic illustration of the preparations of prevascularized cell sheet, PNC, SCI model, and the implantation of PNC into the SCI rat.

2.6. Mechanical measurement

Uniaxial tensile testing was performed for the obtained samples with an electronic universal testing machine (AGS-X 5 KN, Shimadzu, Japan) with 500 N load at a speed of 5 mm min^{-1}.

2.7. SCI model construction

The animal experiments were approved by the Institute's Animal Ethics Committee. Sixty female Sprague Dawley (SD) rats weighing approximately 200 g were randomly divided into three groups, namely, control group, NPNC group, and PNC group, and anesthetized with 10% chloral hydrate (1 mL/250 g). Using eye scissors, the hair on the operational site was removed. The vertebral column was exposed by incising the skin along the midline of the back, followed by T-9 laminectomy under a surgical microscope (Fig. 1). After laminectomy, a segment of the spinal cord with 2 mm length was completely cut and removed. The NPNC and PNC were put into the broken ends to connect the ends. The NC were not sutured to the broken ends; instead, they adhered to the broken ends through the fibronectin secreted from the ECM of the cell sheet. A titanium mesh was used as the immobilized material to provide the necessary protective support, effectively avoiding the secondary trauma caused by the rats' motion (Fig. S1). Nonabsorbable surgical sutures were used to sequentially suture the muscle and skin of the rats. The rats were fed with cyclosporin A at a dose of 5–10 mg/kg every day to inhibit the immunological rejection reaction. The bladder was squeezed twice a day to help in urination until the function of the bladder rehabilitated.

2.8. Behavior assessment

The locomotor behavior was assessed using Basso, Beattie, Bresnahan (BBB) Locomotor Rating Scale [28]. The rats without observable hindlimb movement were scored "0." Those with normal hindlimb movement were scored "21." Before the assessment was done by two blinded observers, the rats were allowed to walk in an open field for 5 min. The whole assessment process lasted until the 8th week.

2.9. H&E staining

The NPNC and PNC were fixed in 4% paraformaldehyde for 30 min, and then, they were sectioned to 5 μm slices to be immersed in hematoxylin for 1 min and stained by eosin for 30 s. Subsequently, the stained slices were washed with water, dehydrated using graded alcohol, cleared in xylene, and sealed for microscopic observation. After completion of the experiment, the rats were perfused with 4% paraformaldehyde. The spinal cord was retrieved from the rats and postfixed in 4% paraformaldehyde solution for another 4 h; and then it was immersed in 30% sucrose solution overnight. The fixed spinal cord was sliced into 15 μm slices, which were further stained by H&E staining.

2.10. Immunohistochemistry staining

The obtained cryosections were firmly attached to the glass slides, and then they were blocked with 1% BSA for 1 h. After that, primary antibodies including mouse anti-CD31, mouse antifibronectin, and mouse anticollagen I were used for the immunohistochemical staining of the prepared neuron conduits. Mouse anti-CD31, mouse anti-Tuj-1, and chicken anti-GFAP were used for the immunohistochemical staining of the repaired spinal neurons. After incubation at room temperature for 2 h, the sections were rinsed thrice with PBS. Secondary antibodies including goat antimouse Alexa Fluor®647 for neuron conduits and spinal neurons and goat antichicken Alexa Fluor®405 for spinal neurons were applied for 1 h at room temperature in the dark. The sections were washed thrice with PBS. The experimental procedure of myelin basic protein (MBP) immunofluorescence staining (mouse anti-MBP) was similar to the above-mentioned methods in addition to the application of DAB as a color-developing reagent. All slides were sealed with the addition of an antifluorescence quenching agent and were observed and imaged using a laser scanning confocal microscope (Olympus FV 1000).

2.11. Luxol fast blue (LFB) staining

The fixed spinal cords were sectioned to 5 μm slices and stained with Luxol fast blue (LFB). Subsequently, the stained slices were washed with water, dehydrated using graded alcohol, cleared in xylene, and sealed for microscopic observation.

2.12. Statistical analysis

All statistical analyses were analyzed using OriginPro 9.0 software. Experimental data were analyzed with Student's *t*-test, in which data were expressed as means ± standard deviations (SD). $p < 0.05$ was considered to indicate significance.

3. Results and discussion

We successfully developed the prevascularized cell sheet to construct NC for SCI repair. Briefly, with an aim to address the issues of ischemia, hypoxia, and the limited regenerative ability of the remained neurons, the innovative idea was to introduce the microvascular networks and MSC resources into the neuron conduits. The prevascularized cell sheet was fabricated based on our previously reported methods by culturing the HUVECs on the preformed stem cell sheet, after the formation of the prevascularized stem cell sheet, which can be easily lifted with the help of the forceps and rolled into the needed tube-like structure (denoted as nerve conduit, NC) by using the PTFE as the model. To assess its

Please cite this article as: Z. Fan, X. Liao and Y. Tian et al., A prevascularized nerve conduit based on a stem cell sheet effectively promotes the repair of transected spinal cord injury, Acta Biomaterialia, https://doi.org/10.1016/j.actbio.2019.10.042

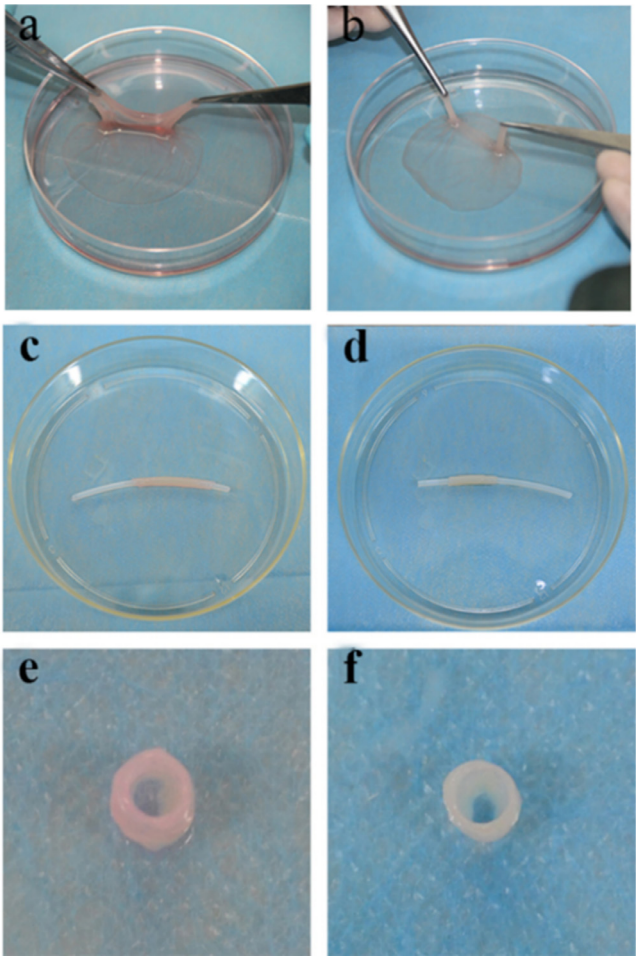

Fig. 2. Photographs of MSC cell sheet (a); prevascularized MSC cell sheet (b); rolling into NPNC based on MSC cell sheet (c); rolling into PNC based on prevascularized MSC cell sheet (d); NPNC based on MSC cell sheet after removal from the PTFE model (e); PNC based on the prevascularized MSC cell sheet after removal from the PTFE model (f).

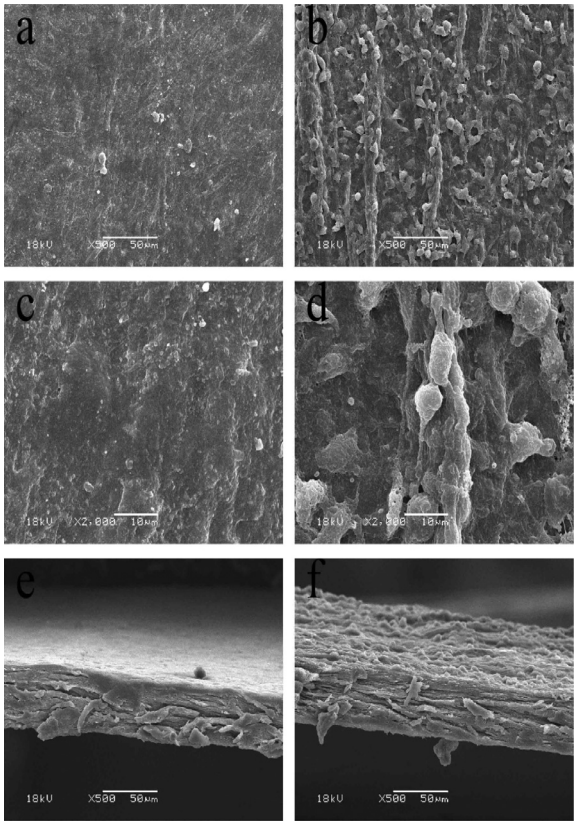

Fig. 3. SEM images of NPNC (a and c) and PNC (b and d) at different magnifications, and the cross profile images of NPNC (e) and PNC (f).

healing effect in different time intervals, the prepared NC was implanted into the SCI rat. The specific marks of MSCs were identified by immunofluorescence staining, including CD 29, CD 44, and CD 90 (Fig. S2). In addition, the differentiation potential of the MSCs was characterized by osteogenic induction, adipogenic introduction, and neurogenic introduction (Fig. S3). The surface of MSCs presented specific markers of rabbit MSCs, including CD 29, CD 44, and CD 90 (Fig. S2), which verified that the obtained MSCs have the characteristics of rabbit MSCs [29, 30] as well as multipotency, which can differentiate into the osteoblasts, adipocytes, and neurons under differently induced conditions (Fig. S3). Ascorbic acid can promote the secretion of ECM and facilitate the self-assembly of the cell sheet [31]. A complete and contiguous cell sheet (Fig. 2a) and prevascularized cell sheet (Fig. 2b) were formed and could be easily lifted from the surface of the petri dish using the forceps. After being rolled as a tubular structure and cultured for another 7 days, the cell sheet could be removed from the PTFE model (Fig. 2c and 2d) and remained complete (Fig. 2e and 2f) depending on the self-supporting mechanical reinforcement. Further confirmation can be found from the mechanical measurement (Fig. S4), and the results showed that the tensile strength of PNC was approximately 1.5 MPa, and the strain could reach 45%. The good mechanical properties of PNC ensure that it could not be broken easily when it was applied at the extension site of the spine. The layers fused together and integrated into an integral structure without noticeable gaps between the layers relying on the fibronectin, which can be further revealed from the results of H&E staining and immunohistochemical staining (Figs. S5 and 4). The average thickness of the MSC cell sheet was approximately 478.5 μm; however, after the formation of the prevascularized MSC cell sheet, the average thickness was reduced to approximately 424.3 μm. Regarding NPNC, the average thickness could reach 3200 μm. After the formation of PNC, the thickness of the NC reduced, and the average thickness was approximately 2800 μm. The reason may be that the prevascularization could have made the cell sheet become tighter, causing reduction in thickness.

The SEM images of the NPNC and PNC are shown in Fig. 3. The cell sheet surface of the NPNC was smooth and surrounded by a large amount of ECM, whereas the cell sheet surface of the PNC became coarser and had many microvessel-like structures, indicating the formation of microvessel networks.

We performed immunohistochemistry staining to further prove the fusion of the cell sheet and prevascularization formation (Fig. 4). It has been reported that collagen I and fibronectin are two kinds of proteins important for cell sheet assembly and fusion [32]. The expression of collagen I protein was almost the same between the NPNC and PNC groups. Differently, the expression of the fibronectin protein in the PNC group was higher than that in the NPNC group; this was why the layers between cell sheet could fuse into a whole and the thickness could present a reduced trend after the formation of prevascularization (Fig. S5d). Further, the arrangement of both proteins became more orderly after the formation of the prevascularized cell sheet (Fig. 4b and d). CD 31 staining was found as a negative result in the NPNC group, while it was positive in the PNC group with the appearance of several lumen with a microvessel-like pattern in the sample (Fig. 4f), showing that prevascularization played an important role in promoting the for-

Please cite this article as: Z. Fan, X. Liao and Y. Tian et al., A prevascularized nerve conduit based on a stem cell sheet effectively promotes the repair of transected spinal cord injury, Acta Biomaterialia, https://doi.org/10.1016/j.actbio.2019.10.042

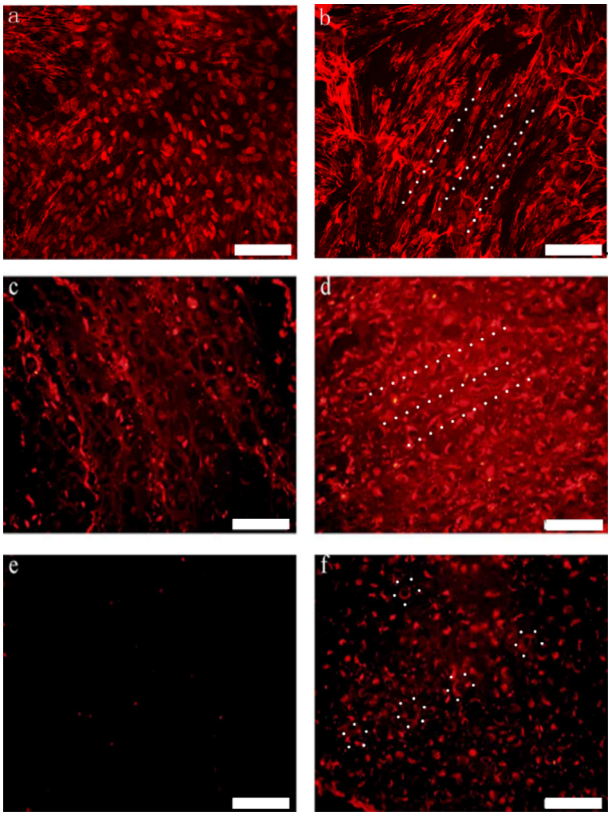

Fig. 4. Immunofluorescence images stained with Collagen I (a, NPNC; b, PNC), Fibronectin (c, NPNC; d, PNC), and CD31 (e, NPNC; f, PNC). The white lines denote the ordered arrangement of related proteins. The white circles denote the microvessel (scale bar = 200 μm). (For interpretation of the references to colour in this figure legend, the reader is referred to the web version of this article.)

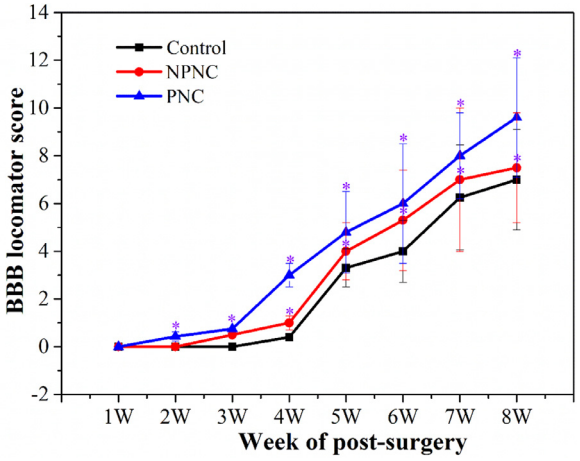

Fig. 5. BBB scores: BBB scores of the control group, NPNC group, and PNC group (*: $P<0.05$ vs. blank group).

mation of the microvessel-like pattern by co-culturing MSCs with ECs. The importance of prevascularization has been confirmed in many studies. For example, in the study by Yang et al., to construct vascularized bone grafts, the prevascularized cell sheet was used as the biomimetic periosteum, which could enhance angiogenesis and functional anastomosis between the in vitro preformed human capillary networks and the mouse host vasculature [33]. For the treatment of large bone defects, Ren et al. applied the prevascularized cell sheet as the biomimetic induced membrane, verifying that the constructed composite membrane showed rapid vascularization and anastomosis with the host vascular system and formed functional blood vessels *in vivo* [34]. As mentioned above, the introduction of microvessels in the PNC can promote microvessel reconstruction and anastomosis with the host vascular system, hoping that it can address the issues of ischemia and hypoxia in the rehabilitation of SCI.

In this study, heterogeneous cells were used to repair the SCI of SD rats, which may cause immunogenicity. To avoid immunological rejection, the animals were fed with cyclosporin A, an immunosuppressant that is widely used to prevent rejection in response to organ transplantation. Furthermore, we implanted the prevascularized cell sheet into the subcutaneous pocket of the SD rats to observe the growth status of the cell sheet and inflammatory reaction through H&E staining. The results showed that the PNC group formed more microvessels than the NPNC group in the 2nd and the 4th week, and we also observed that the NPNC group and the PNC group had a lower inflammatory reaction, indicating the introduction of human ECs had no or low immunoreactivity to the host animal (Fig. S6). The reason may be that the MSCs secreted an amount of ECM that could enclose the human ECs, leading to a decrease in the immunogenicity. On the basis of low immunoreactivity, the NPNC group and the PNC group were implanted into the area of SCI of SD rats to observe the healing effect in vivo. To quantify the repair efficiency of SCI, BBB score is an effective option. The BBB score in the PNC group (Fig. 5) was higher than that in the control group with a statistically significant difference ($p<0.05$) from the 2nd week. However, no statistically significant difference could be observed between the NPNC group and the control group within 4 weeks. From the 4th week, the BBB score in the PNC group was far higher than that in the NPNC and control groups, indicating that prevascularization can accelerate the repair process of SCI. To record the healing effect, we captured videos. For rats in the control group, the hind limbs could not be moved even after 8 weeks (Supporting Information, Video S1). For the rats treated with NPNC, partial movement was recovered and the hind limbs of the rat could swing back and forth (Supporting Information, Video S2). As we have predicted before, the rats treated with PNC could crawl on the ground depending on the support of its hind limbs (Supporting Information, Video S3).

The photographs of the spinal cord are shown in Fig. S7. In the 2nd week, the damaged area of the control group presented obvious atrophy (Fig. S7a), but there was no atrophy in the NPNC and PNC groups (Fig. S7b and c). In the 8th week, there was slight atrophy in the control group (Fig. S7d). In contrast, the NPNC showed a swelling trend (Fig. S7e). Completely different from the control and NPNC groups, neither atrophy nor swelling appeared in the damaged area after treatment with PNC (Fig. S7f).

The foregoing morphological observations can be further substantiated by H&E staining (Fig. 6). In the 2nd week, the control group showed significant atrophy and the surrounding tissues of the lesion area became looser; in addition, many inflammatory cells infiltrated into the damaged area (Fig. 6a). For NPNC, there was slight atrophy, and the damaged area and its surrounding tissues were filled with inflammatory cells. A portion of the cell sheet did not fuse with its surrounding tissues (Fig. 6b). The PNC group did not present noticeable atrophy, and the inflammatory response in this group was lower than that in the control group and the NPNC group. Further, the cell sheet completely fused with its surrounding tissues (Fig. 6c). In the 8th week, slight atrophy could be observed in the control group, and although the inflammatory cells remained, their number was less than that in the 2nd week (Fig. 6d). The morphology of NPNC recovered to its previous volume, some inflammatory cells remained, and the cell sheet did not completely fuse with its surrounding tissue (Fig. 6e). When compared with the control and NPNC groups, the PNC group did not

Please cite this article as: Z. Fan, X. Liao and Y. Tian et al., A prevascularized nerve conduit based on a stem cell sheet effectively promotes the repair of transected spinal cord injury, Acta Biomaterialia, https://doi.org/10.1016/j.actbio.2019.10.042

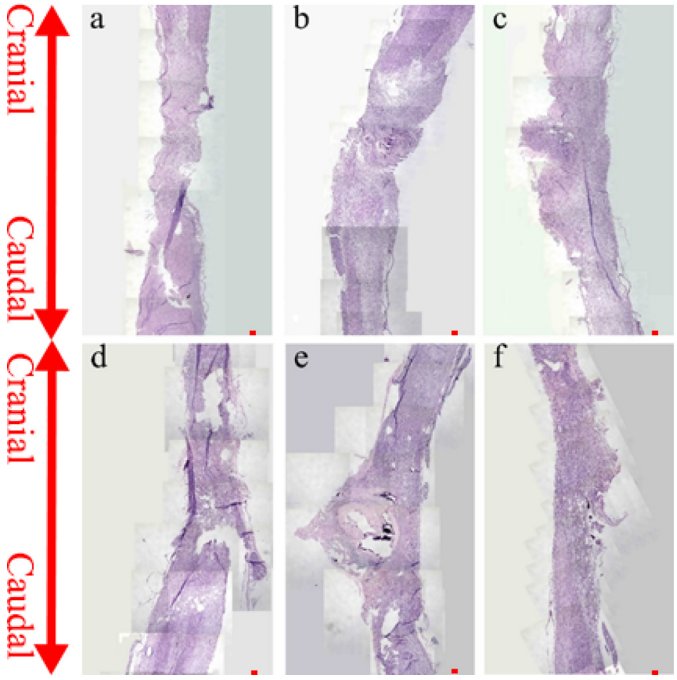

Fig. 6. Light microscopic images of H&E staining. a, Control group at 2 weeks; b, NPNC group at 2 weeks; c, PNC group at 2 weeks; d, Control group at 8 weeks; e, NPNC group at 8 weeks; f, PNC group at 8 weeks (scale bar = 100 μm).

have noticeable atrophy, and fewer inflammatory cells infiltrated into the damaged area (Fig. 6f).

In addition to the overall observation of H&E staining, local observations was also done by magnifying the repair location (Figs. 7 and S8). In the 2nd week, relatively fewer neurons appeared around the repair area of the control group (Figs. 7a and S8a). In contrast, when treated with NPNC and PNC, the repair area contained many neurons, which may be derived from the induced differentiation of MSCs in vivo. Moreover, further validation was provided in subsequent immunohistochemistry experiments (Figs. 9b and 9c). Further, we could observe some small nerve fibers appearing in the repair area in the 2nd week. Compared to the other two groups, more nerve fibers could be observed in the PNC group (Figs. 7c and S8c). In addition, more vacuoles appeared in the control group than in the other two groups (Figs. 7a and S8a). At the 8th week, more vacuoles remained in the control group than in the other two groups (Figs. 7d and S8d). Moreover, a decreasing trend in the number of neurons but an increasing trend in the number of nerve fibers could be observed. The nerve fibers of the control group were less in number, smaller, and more disordered than those of the other two experimental groups (Figs. 7d and S8d). After treatment with NPNC, the nerve fibers presented a more orderly arrangement than those of the control group (Figs. 7e and S8e). When the prevascularized network was introduced into the NC, the nerve fibers became thicker, longer, and more orderly than those of the other two groups (Figs. 7f and S8f). Among the three groups, more astrocytes appeared in the control group, which were clearly associated with the formation of the glial scar [35]. As mentioned above, the introduction of vascularized networks into the NC can be approved to effectively improve the healing of the damaged spinal cord by decreasing the inflammatory response, promoting the formation of more neurons, and inhibiting the proliferation of astrocytes.

Prevascularization is vital to sustaining the survival of the cells around the damaged area by supplying sufficient nutrients and oxygen [36]. The prevascularization effect can be quantified by the CD31 immunohistochemistry because CD31 is a biomarker of ECs [37]. In the 2nd week, the expression of CD31 in the control group was the least among the three groups (Figs. 8a and 8g). Although the expression in both experimental groups was almost the same, it was higher than that of the control group (Fig. 8b–c and 8 g). At the time point of 8th week, the expression of CD31 dramatically decreased in the control group as compared to the counterpart of the 2nd week. However, a significant increase in the expression can be observed in both experimental groups. It was revealed that the PNC group had the highest expression among the three groups (Figs. 8f and S8a), which indicated that prevascularization was an effective way to promote the vascularization of the grafted NC, sustain its survival, and finally resolve the issues of ischemia and hypoxia, which are the two key issues a challenge in the SCI therapy. The prevascularized cell sheet has been proven to play an important role in repairing the bone and skin tissues as determined by the supply of necessary nutrients and oxygen, enabling to promote the survival of transplanted tissues [38,39]. However, as to neuron repair, there are no related reports. Therefore, our research not only first proved the important role of the prevascularized cell sheet in SCI repair but also paved the way for expanding the application of prevascularized cell sheet in SCI repair.

A neuron-specific beta III microtubule, termed Tuj-1, was thought to be one of the earliest biomarkers of stem cell differentiation to neurons, whose antibodies are often used to mark the early stages of neuron differentiation [40]. Glial fibrillary acidic protein (GFAP) is one of the best biomarkers for the activation of astrocytes following injury or stress in the central nervous system [41]. Therefore, these two kinds of proteins were analyzed by immunohistochemistry, and the corresponding results are shown in Figs. 9 and 10; in the 2nd week, the expression of Tuj-1 in the control group was lower than that in both experimental groups (Figs. 9a, S10a, and S12a), while it was significantly increased after the addition of MSCs and almost similar to each other (Figs. 9b, 9c, S10b, S10c, and S12a). With prolonging time to the 8th week, the expression of Tuj-1 in the control group showed a slight increase but was still lower than that in both experimental groups (Figs. 9d, S10d, and S12a). In contrast, the expression of Tuj-1 in both experimental groups increased dramatically (Figs. 9e, 9f, S10e, S10f, and S12a). Noticeably, the expression of Tuj-1 in the PNC group was the highest as compared to that of the other two groups (Figs. 9f, S10f, and S12a). There may be three reasons for enhancing the expression of Tuj-1. The first reason is that some neonatal neurons probably come from the differentiation of MSCs. The second reason is that some neonatal neurons may be derived from the local neurons of the spinal cord because the gap between both broken ends is so short that the local neurons of the spinal cord can migrate to the defect site (Fig. 9d). The third reason is that the preformed microvessels can provide ample oxygen and nutrition, sustaining the survivor of the neonatal neurons. To determine the detailed mechanism, immunofluorescence tracking methods can be used in further study to determine where the neonatal neurons come from. As to the GAFP expression, a contrasting trend could be observed as compared to that of Tuj-1. In the 2nd week, the highest expression appeared in the control group (Figs. 10a, S11a, and S12b). The expression in both experimental groups was almost the same but was lower than that of the control group (Figs. 10b, 10c, S11b, S11c, and S12b). In the 8th week, the expression of GAFP in the control group exhibited a significantly increasing trend (Figs. 10d, S11d, and S12b). Conversely, a slightly increasing trend of GAFP could be observed in both experimental groups, but it was still far lower than that of the control group (Figs. 10e, 10f, S11e, S11f, and S12b).

We also quantified the expression of myelin by MBP immunofluorescence staining and LFB staining in the 8th week, and the corresponding results are shown in Figs. S13 and S14. As shown in Fig. S13a, MBP staining in the control group presented a spot-

Please cite this article as: Z. Fan, X. Liao and Y. Tian et al., A prevascularized nerve conduit based on a stem cell sheet effectively promotes the repair of transected spinal cord injury, Acta Biomaterialia, https://doi.org/10.1016/j.actbio.2019.10.042

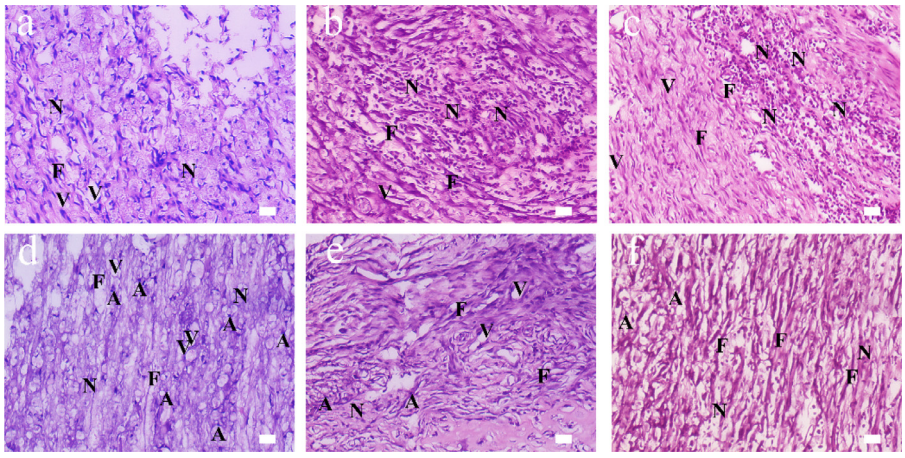

Fig. 7. H&E staining images of the injured site. a, Control group at 2 weeks; b, NPNC group at 2 weeks; c, PNC group at 2 weeks; d, Control group at 8 weeks; e, NPNC group at 8 weeks; f, PNC group at 8 weeks. A, denotes the astrocyte; F, denotes the neuron; N, denotes the neuron fibers; V, denotes the vacuole (scale bar = 200 μm). (For interpretation of the references to colour in this figure legend, the reader is referred to the web version of this article.)

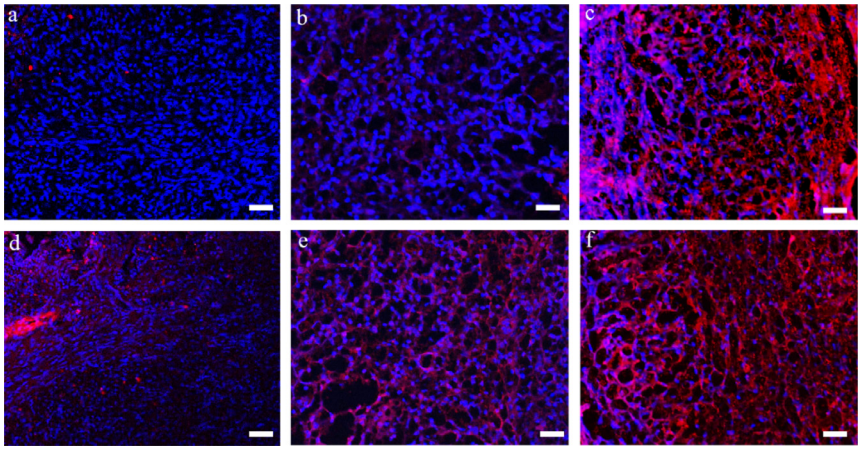

Fig. 8. Images of CD31 immunofluorescence staining; CD31 is marked with red fluorescence, and cell nuclei are marked with blue fluorescence. a, Control group at 2 weeks; b, NPNC group at 2 weeks; c, PNC group at 2 weeks; d, Control group at 8 weeks; e, NPNC group at 8 weeks; f, PNC group at 8 weeks (scale bar = 100 μm). (For interpretation of the references to colour in this figure legend, the reader is referred to the web version of this article.)

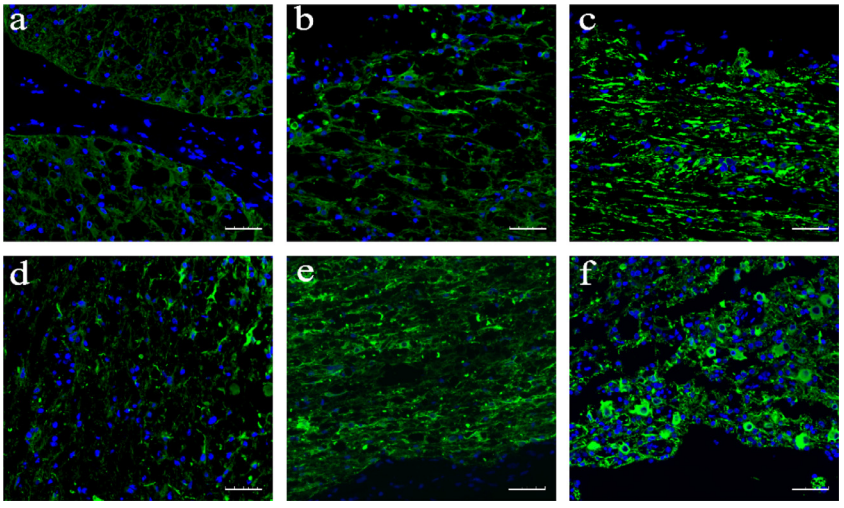

Fig. 9. Images of Tuj-1 immunofluorescence staining; Tuj-1 is marked in green color, and while cell nuclei are marked in blue color. a, Control group at 2 weeks; b, NPNC group at 2 weeks; c, PNC group at 2 weeks; d, Control group at 8 weeks; e, NPNC group at 8 weeks; f, PNC group at 8 weeks (scale bar = 250 μm). (For interpretation of the references to colour in this figure legend, the reader is referred to the web version of this article.)

Please cite this article as: Z. Fan, X. Liao and Y. Tian et al., A prevascularized nerve conduit based on a stem cell sheet effectively promotes the repair of transected spinal cord injury, Acta Biomaterialia, https://doi.org/10.1016/j.actbio.2019.10.042

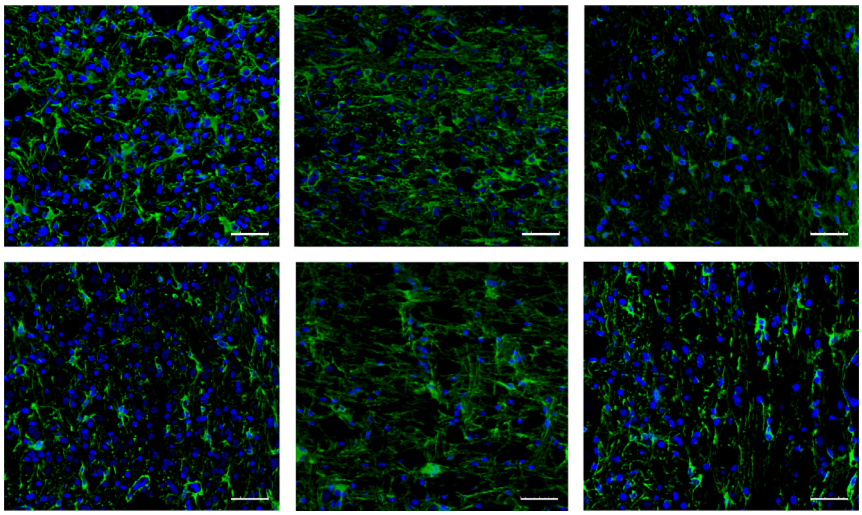

Fig. 10. Images of GFAP immunofluorescence staining. GFAP is marked in green color, and while cell nuclei are marked in blue color. a, Control group at 2 weeks; b, NPNC group at 2 weeks; c, PNC group at 2 weeks; d, Control group at 8 weeks; e, NPNC group at 8 weeks; f, PNC group at 8 weeks (scale bar = 250 μm). (For interpretation of the references to colour in this figure legend, the reader is referred to the web version of this article.)

like pattern, and the number of myelinated axons was the least (Fig. S14a), indicating that severe demyelination still existed in the control group. However, when the rats were treated with NPNC and PNC, a linear staining pattern of MBP rather than a spot-like pattern was observed (Figs. S13b and S13c), and the number of myelinated axons in both groups was higher than that of the control group (Fig. S14a). Among the three groups, the PNC group had the highest number of myelinated axons (Fig. S14a), and the linear staining pattern of MBP in this group was more obvious (Fig.. S13c), implying more MBP regeneration in this group. In the LFB staining, the staining area in the PNC group was larger than that in the other two groups (Figs. S13f and S14b), further confirming the regeneration of more myelinated axons in the PNC group. The results of Tuj-1 immunofluorescence staining and myelin staining confirm that more new neurons come from the differentiation of BMSCs are involved in the SCI repair.

Some research confirms that the expression of GFAP is considered to be negatively correlated with the formation of the inhibitory glial scar. Thus, the reduction in the expression of GFAP is more desirable for the SCI repair [42,43]. After SCI, the astrocytes show hypertrophy, hyperplasia, and reactive gliosis, leading to the formation of the glial scar. In the early stage, the astrocytes can fill the damaged area and prevent the change in the spinal cord morphology, which can play the role of a scaffold [44]. The glial scar secreted by the astrocytes can also protect the neural tissues. In the late stage, the astrocytes have an inhibitory effect on neural development. The formation of the glial scar will affect the regeneration and growth of axons [45]. In the H&E staining, the number of astrocytes in the control group was higher than that of the other two experimental groups, which was consistent with the results of immunohistochemistry (Figs. 7, 10a, and 10d). Further, the poorest healing effect appeared in the control group, implying that the GFAP expressed by astrocytes had an inhibitory effect on the neural development.

SCI repair is a huge challenge faced by clinical medicine, and how to improve the repair effect is scientists' unswerving pursuit. Presently, stem cell therapy and composite scaffolds are commonly used. Stem cell therapy was known to be an effective method in the rehabilitation of SCI for their multipotency [46]. Particularly, stem cell injection is being commonly used, which can be introduced into the defect site through intravenous injection; however, the repair effect was unsatisfactory because of the existing drawbacks including the clearance of MSCs in the immune system and the loss of MSCs in the injection site [47]. To overcome the drawbacks of MSC injection, the composite scaffolds composed of MSCs and scaffold materials were an alternative method to MSC injection. The problems of scaffold materials lie in the immunogenicity, uncontrollable degradation, and acid production in the process of degradation [48]. In addition, there was limited repair effect for most reported composite scaffolds lacked a hollow structure so that it was very difficult to allow the axon to freely grow. With the advancement of research, an increasing number of scientists began to realize that NC was an effective method in the rehabilitation of SCI because it could not only provide bridging between both ends of the nerve defect but also provide guidance cues to the regeneration of the nerve defect [49,50]. Therefore, this method was considered an ideal repair method for the rehabilitation of SCI. To obtain a better repair effect, various molecular cues were introduced into the NC, such as nerve growth factors (NGFs), brain-derived neurotrophic factor (BDNF), and steroid [51,52]. Although a large number of methods were used by researchers to construct the NC, the above-mentioned key limiting factors of SCI repair remained neglected in their studies. With an aim to overcome the existing drawbacks in the MSC injection and scaffold material application, we originally used the cell sheet, composed of MSCs, ECs, and their secreted ECM, as a new repair material for SCI rehabilitation. The MSCs in the cell sheet have the multipotency, which can be differentiated into neurons in vivo and resolve the problem of limited regeneration of the remained neurons in the defect site (Figs. S2, S3, and 9). The ECM not only had good biocompatibility and biodegradation but also contained various growth factors that were beneficial to nerve regeneration, avoiding the addition of molecular cues [53,54]. As an important constituent of ECM, fibronectin was highly expressed in the PNC group than in the control group and the NPNC group and arranged along with a fixed orientation (Figs. 4c and d). Numerous studies have highlighted that the fibronectin expressed in distinct spatial and temporal patterns benefits the natural healing processes of the nervous system [55], which may be one reason why the PNC can promote the healing of transected SCI. More importantly, we introduced microvessels in the NC by co-culturing ECs and MSCs, ensuring the permeability of NC and providing the necessary blood, oxygen, and nutrition supply to the cells present in nerve tissues, thereby successfully resolving the two key issues faced by SCI repair (Figs. 3, 4, and 8). Thus, a more ideal repair effect is generated (Fig. 5 and Video S3). When compared with some injection methods, the BBB

Please cite this article as: Z. Fan, X. Liao and Y. Tian et al., A prevascularized nerve conduit based on a stem cell sheet effectively promotes the repair of transected spinal cord injury, Acta Biomaterialia, https://doi.org/10.1016/j.actbio.2019.10.042

score in the 8th week in our study was higher than some reported value [56,57]. Similarly, the BBB score was also higher than some reported value by using the methods of scaffold materials [58,59], showing that the introduction of microvessels in the NC is an effective way to promote the repair of transected SCI.

Although a better repair effect was obtained, there was much scope for enhancing the healing effect of SCI, including the introduction of growth factor delivery carriers, improvement in the maturity and stability of microvessels, and application of electric stimulation. In addition, further studies on the repair mechanism based on molecular biology and the role of stem cells in the regeneration of the nerve are needed. As much more attention is paid to the prevascularized NC, more healing effect on SCI repair will be achieved to eventually recover the motor and sensory function of patients with SCI to improve their life quality.

4. Conclusions

With an aim to resolve the challenges of ischemia and hypoxia faced by SCI repair, new NC based on the prevascularized cell sheet were fabricated, which can supply sufficient nutrition and oxygen to sustain the survival of the transplanted cell sheet and its surrounding host damage tissues. More importantly, they can effectively enhance the BBB score and promote a higher expression of Tuj-1 than that in the control group and the MSC cell sheet group, indicating their better repair effect on SCI. The novel conduits not only provide a new therapeutic method for SCI but also expand the application range of the cell sheet.

Declaration of Competing Interest

The authors declare that they have no known competing financial interests or personal relationships that could have appeared to influence the work reported in this paper.

Acknowledgment

We deeply appreciate the support from the National Natural Science Foundation of China (81571829); the Medical Subject Fund of Stomatology College of Lanzhou University (201502-3); the Fundamental Research Funds for the Central Universities (861843); the open project of State Key Laboratory of Solid Lubrication, Lanzhou Institute of Chemical Physics, Chinese Academy of Sciences (LSL-1505); the Fundamental Research Funds for the Central Universities (lzujbky-2017-145 and lzujbky-2017-it47); and the Cooperative Project between Gansu Academy of Sciences and Chinese Academy of Sciences (2016HZ_03).

Supplementary materials

Supplementary material associated with this article can be found, in the online version, at doi:10.1016/j.actbio.2019.10.042.

References

[1] N.A. Silva, N. Sousa, R.L. Reis, A.J. Salgado, From basics to clinical: a comprehensive review on spinal cord injury, Prog. Neurobiol. 114 (2014) 25–57.
[2] S. Liu, T. Schackel, N. Weidner, R. Puttagunta, Biomaterial-Supported cell transplantation treatments for spinal cord injury: challenges and perspectives, Front. Cell Neurosci. 11 (430) (2018) 1–19.
[3] D.P. Ankeny, P.G. Popovich, Mechanisms and implications of adaptive immune responses after traumatic spinal cord injury, Neuroscience 158 (3) (2009) 1112–1121.
[4] Charles H. Tator, Michael G. Fehlings, Review of the secondary injury theory of acute spinal cord trauma with emphasis on vascular mechanisms, J. Neurosurg. 75 (1) (1991) 15–26.
[5] O.J. Achadu, J. Britton, T. Nyokong, Graphene quantum dots functionalized with 4-Amino-2, 2, 6, 6-Tetramethylpiperidine-N-Oxide as fluorescence "Turn-ON" nanosensors, J. Fluoresc. 26 (6) (2016) 2199–2212.
[6] Y. Sekine, C.S. Siegel, T. Sekine-Konno, W.B.J. Cafferty, S.M. Strittmatter, The nociceptin receptor inhibits axonal regeneration and recovery from spinal cord injury, Sci. Signal 11 (524) (2018) 1–12.
[7] H. Wang, Y. Wang, D. Li, Z. Liu, Z. Zhao, D. Han, Y. Yuan, J. Bi, X. Mei, VEGF inhibits the inflammation in spinal cord injury through activation of autophagy, Biochem. Biophys. Res. Commun. 464 (2) (2015) 453–458.
[8] Y. Yun, J. Oh, Y. Kim, G. Kim, M. Lee, Y. Ha, Characterization of neural stem cells modified with hypoxia/neuron-specific VEGF expression system for spinal cord injury, Gene. Ther. 25 (2017) 27–38.
[9] S. Yu, S. Yao, Y. Wen, Y. Wang, H. Wang, Q. Xu, Angiogenic microspheres promote neural regeneration and motor function recovery after spinal cord injury in rats, Sci. Rep. 6 (2016) 1–13.
[10] H. Iwai, H. Shimada, S. Nishimura, Y. Kobayashi, G. Itakura, K. Hori, K. Hikishima, H. Ebise, N. Negishi, S. Shibata, Allogeneic neural stem/progenitor cells derived from embryonic stem cells promote functional recovery after transplantation into injured spinal cord of nonhuman primates, Stem. Cells Transl. Med. 4 (7) (2015) 708–719.
[11] K. Kikuchi, H. Yoshimatsu, M. Mihara, M. Narushima, T. Iida, I. Koshima, Vascularized nerve flap for spinal cord repair—a preliminary study, Eplasty 11 (2011) 106–115.
[12] C.P. Hofstetter, E.J. Schwarz, D. Hess, J. Widenfalk, A. El Manira, D.J. Prockop, L. Olson, Marrow stromal cells form guiding strands in the injured spinal cord and promote recovery, Proc. Natl. Acad. Sci. 99 (4) (2002) 2199–2204.
[13] T.S. Wilems, J. Pardieck, N. Iyer, S.E. Sakiyama-Elbert, Combination therapy of stem cell derived neural progenitors and drug delivery of anti-inhibitory molecules for spinal cord injury, Acta Biomater. 28 (2015) 23–32.
[14] S. Vadivelu, T.J. Stewart, Y. Qu, K. Horn, S. Liu, Q. Li, J. Silver, J.W. McDonald, NG2+ progenitors derived from embryonic stem cells penetrate glial scar and promote axonal outgrowth into white matter after spinal cord injury, Stem. Cells Transl. Med. 4 (4) (2015) 401–411.
[15] P. Lu, G. Woodruff, Y. Wang, L. Graham, M. Hunt, D. Wu, E. Boehle, R. Ahmad, G. Poplawski, J. Brock, Lawrence S.B. Goldstein, Mark H. Tuszynski, Long-Distance axonal growth from human induced pluripotent stem cells after spinal cord injury, Neuron 83 (4) (2014) 789–796.
[16] N.R. Iyer, T.S. Wilems, S.E. Sakiyama-Elbert, Stem cells for spinal cord injury: strategies to inform differentiation and transplantation, Biotechnol. Bioeng. 114 (2) (2017) 245–259.
[17] R.S. Oliveri, S. Bello, F. Biering-Sørensen, Mesenchymal stem cells improve locomotor recovery in traumatic spinal cord injury: systematic review with meta-analyses of rat models, Neurobiol. Dis. 62 (2014) 338–353.
[18] I. Caron, F. Rossi, S. Papa, R. Aloe, M. Sculco, E. Mauri, A. Sacchetti, E. Erba, N. Panini, V. Parazzi, M. Barilani, G. Forloni, G. Perale, L. Lazzari, P. Veglianese, A new three dimensional biomimetic hydrogel to deliver factors secreted by human mesenchymal stem cells in spinal cord injury, Biomaterials 75 (2016) 135–147.
[19] D. Tukmachev, S. Forostyak, Z. Koci, K. Zaviskova, I. Vackova, K. Vyborny, I. Sandvig, A. Sandvig, C.J. Medberry, S.F. Badylak, Injectable extracellular matrix hydrogels as scaffolds for spinal cord injury repair, Tissue Eng. Part A 22 (3–4) (2016) 306–317.
[20] T. Owaki, T. Shimizu, M. Yamato, T. Okano, Cell sheet engineering for regenerative medicine: current challenges and strategies, Biotechnol. J. 9 (7) (2014) 904–914.
[21] T. Iwata, K. Washio, T. Yoshida, I. Ishikawa, T. Ando, M. Yamato, T. Okano, Cell sheet engineering and its application for periodontal regeneration, J. Tissue Eng. Regen. Med. 9 (4) (2015) 343–356.
[22] Y. Kato, T. Iwata, S. Morikawa, M. Yamato, T. Okano, Y. Uchigata, Allogeneic transplantation of an adipose-derived stem cell sheet combined with artificial skin accelerates wound healing in a rat wound model of type 2 diabetes and obesity, Diabetes 64 (8) (2015) 2723–2734.
[23] N. Itaba, Y. Matsumi, K. Okinaka, A.A. Ashla, Y. Kono, M. Osaki, M. Morimoto, N. Sugiyama, K. Ohashi, T. Okano, G. Shiota, Human mesenchymal stem cell-engineered hepatic cell sheets accelerate liver regeneration in mice, Sci. Rep. 5 (2015) 1–17.
[24] O. Ishida, I. Hagino, N. Nagaya, T. Shimizu, T. Okano, Y. Sawa, H. Mori, T. Yagihara, Adipose-derived stem cell sheet transplantation therapy in a porcine model of chronic heart failure, Transl. Res. 165 (5) (2015) 631–639.
[25] J.Á.P. Gomes, B.G. Monteiro, G.B. Melo, R.L. Smith, M.C.P. da Silva, N.F. Lizier, A. Kerkis, H. Cerruti, I. Kerkis, Corneal reconstruction with tissue-engineered cell sheets composed of human immature dental pulp stem cells, Invest. Ophthalmol. Vis. Sci. 51 (3) (2010) 1408–1414.
[26] L. Zhang, Q. Xing, Z. Qian, M. Tahtinen, Z. Zhang, E. Shearier, S. Qi, F. Zhao, Hypoxia created human mesenchymal stem cell sheet for prevascularized 3D tissue construction, Adv. Healthc. Mater. 5 (3) (2016) 342–352.
[27] J. Chen, D. Zhang, Q. Li, D. Yang, Z. Fan, D. Ma, L. Ren, Effect of different cell sheet ECM microenvironment on the formation of vascular network, Tissue Cell 48 (5) (2016) 442–451.
[28] B.J. Cummings, N. Uchida, S.J. Tamaki, D.L. Salazar, M. Hooshmand, R. Summers, F.H. Gage, A.J. Anderson, Human neural stem cells differentiate and promote locomotor recovery in spinal cord-injured mice, Proc. Natl. Acad. Sci. U.S.A. 102 (39) (2005) 14069–14074.
[29] T.L. Ramos, L.I. Sánchez-Abarca, S. Muntión, S. Preciado, N. Puig, G. López-Ruano, Á. Hernández-Hernández, A. Redondo, R. Ortega, C. Rodríguez, MSC surface markers (CD44, CD73, and CD90) can identify human MSC-derived extracellular vesicles by conventional flow cytometry, Cell Commun. Signal. 14 (1) (2016) 1–14.

Please cite this article as: Z. Fan, X. Liao and Y. Tian et al., A prevascularized nerve conduit based on a stem cell sheet effectively promotes the repair of transected spinal cord injury, Acta Biomaterialia, https://doi.org/10.1016/j.actbio.2019.10.042

[30] S.L. Tan, T.S. Ahmad, L. Selvaratnam, T. Kamarul, Isolation, characterization and the multi-lineage differentiation potential of rabbit bone marrow-derived mesenchymal stem cells, J. Anat. 222 (4) (2013) 437–450.
[31] P. Guo, J.j. Zeng, N. Zhou, A novel experimental study on the fabrication and biological characteristics of canine bone marrow mesenchymal stem cells sheet using vitamin C, Scanning 37 (1) (2015) 42–48.
[32] Y. Kang, L. Ren, Y. Yang, Engineering vascularized bone grafts by integrating a biomimetic periosteum and β-TCP scaffold, ACS Appl. Mater. Interfaces 6 (12) (2014) 9622–9633.
[33] L. Ren, Y. Kang, C. Browne, J. Bishop, Y. Yang, Fabrication, vascularization and osteogenic properties of a novel synthetic biomimetic induced membrane for the treatment of large bone defects, Bone 64 (2014) 173–182.
[34] Q. Xing, K. Yates, M. Tahtinen, E. Shearier, Z. Qian, F. Zhao, Decellularization of fibroblast cell sheets for natural extracellular matrix scaffold preparation, Tissue Eng. Part C Methods 21 (1) (2014) 77–87.
[35] M.V. Sofroniew, H.V. Vinters, Astrocytes: biology and pathology, Acta Neuropathol. 119 (1) (2010) 7–35.
[36] W. Zhang, L.S. Wray, J. Rnjak-Kovacina, L. Xu, D. Zou, S. Wang, M. Zhang, J. Dong, G. Li, D.L. Kaplan, X. Jiang, Vascularization of hollow channel-modified porous silk scaffolds with endothelial cells for tissue regeneration, Biomaterials 56 (2015) 68–77.
[37] M.P. Pusztaszeri, W. Seelentag, F.T. Bosman, Immunohistochemical expression of endothelial markers CD31, CD34, von Willebrand factor, and Fli-1 In normal human tissues, J. Histochem. Cytochem. 54 (4) (2006) 385–395.
[38] M.A. Kuss, S. Wu, Y. Wang, J.B. Untrauer, W. Li, J.Y. Lim, B. Duan, Prevascularization of 3D printed bone scaffolds by bioactive hydrogels and cell co-culture, J. Biomed. Mater. Res. Part B Appl. Biomater. 106 (5) (2018) 1788–1798.
[39] L. Chen, Q. Xing, Q. Zhai, M. Tahtinen, F. Zhou, L. Chen, Y. Xu, S. Qi, F. Zhao, Pre-vascularization enhances therapeutic effects of human mesenchymal stem cell sheets in full thickness skin wound repair, Theranostics 7 (1) (2017) 117–131.
[40] R. Lee, I.S. Kim, N. Han, S. Yun, K.I. Park, K.H. Yoo, Real-time discrimination between proliferation and neuronal and astroglial differentiation of human neural stem cells, Sci. Rep. 4 (2014) 1–6.
[41] S. Zhang, M. Wu, C. Peng, G. Zhao, R. Gu, GFAP expression in injured astrocytes in rats, Exp. Ther. Med. 14 (3) (2017) 1905–1908.
[42] M. Brenner, Role of GFAP in CNS injuries, Neurosci. Lett. 565 (2014) 7–13.
[43] M. Ribotta, V. Menet, A. Privat, Glial scar and axonal regeneration in the CNS: lessons from GFAP and vimentin transgenic mice, mechanisms of secondary brain damage from Trauma and Ischemia, Springer (2004) 87–92.
[44] D. Sun, T.C. Jakobs, Structural remodeling of astrocytes in the injured CNS, The Neuroscientist 18 (6) (2012) 567–588.
[45] M. Pekny, M. Pekna, Reactive gliosis in the pathogenesis of CNS diseases, Biochimica et Biophysica Acta (BBA) - Mol. Basis Dis. 1862 (3) (2016) 483–491.
[46] V. Sahni, J.A. Kessler, Stem cell therapies for spinal cord injury, Nat. Rev. Neurol. 6 (7) (2010) 363–372.
[47] Y. Haraguchi, T. Shimizu, T. Sasagawa, H. Sekine, K. Sakaguchi, T. Kikuchi, W. Sekine, S. Sekiya, M. Yamato, M. Umezu, Fabrication of functional three-dimensional tissues by stacking cell sheets in vitro, Nat. Protoc. 7 (5) (2012) 850–858.
[48] J. Yang, M. Yamato, C. Kohno, A. Nishimoto, H. Sekine, F. Fukai, T. Okano, Cell sheet engineering: recreating tissues without biodegradable scaffolds, Biomaterials 26 (33) (2005) 6415–6422.
[49] B. Battiston, S. Geuna, M. Ferrero, P. Tos, Nerve repair by means of tubulization: literature review and personal clinical experience comparing biological and synthetic conduits for sensory nerve repair, Microsurgery 25 (4) (2005) 258–267.
[50] J. Mohammad, J. Shenaq, E. Rabinovsky, S. Shenaq, Modulation of peripheral nerve regeneration: a tissue-engineering approach. The role of amnion tube nerve conduit across a 1-centimeter nerve gap, Plast. Reconstr. Surg. 105 (2) (2000) 660–666.
[51] B.S. Bregman, M. McAtee, H.N. Dai, P.L. Kuhn, Neurotrophic factors increase axonal growth after spinal cord injury and transplantation in the adult rat, Exp. Neurol. 148 (2) (1997) 475–494.
[52] M.H. Tuszynski, K. Gabriel, F.H. Gage, S. Suhr, S. Meyer, A. Rosetti, Nerve growth factor delivery by gene transfer induces differential outgrowth of sensory, motor, and noradrenergic neurites after adult spinal cord injury, Exp. Neurol. 137 (1) (1996) 157–173.
[53] T. Iwata, M. Yamato, H. Tsuchioka, R. Takagi, S. Mukobata, K. Washio, T. Okano, I. Ishikawa, Periodontal regeneration with multi-layered periodontal ligament-derived cell sheets in a canine model, Biomaterials 30 (14) (2009) 2716–2723.
[54] S. Masuda, T. Shimizu, M. Yamato, T. Okano, Cell sheet engineering for heart tissue repair, Adv. Drug Deliv. Rev. 60 (2) (2008) 277–285.
[55] S.L. Rogers, P.C. Letourneau, S.L. Palm, J. McCarthy, L.T. Furcht, Neurite extension by peripheral and central nervous system neurons in response to substratum-bound fibronectin and laminin, Dev. Biol. 98 (1) (1983) 212–220.
[56] P. Lu, Y. Wang, L. Graham, K. McHale, M. Gao, D. Wu, J. Brock, A. Blesch, E.S. Rosenzweig, L.A. Havton, Long-distance growth and connectivity of neural stem cells after severe spinal cord injury, Cell 150 (6) (2012) 1264–1273.
[57] Y.D. Teng, E.B. Lavik, X. Qu, K.I. Park, J. Ourednik, D. Zurakowski, R. Langer, E.Y. Snyder, Functional recovery following traumatic spinal cord injury mediated by a unique polymer scaffold seeded with neural stem cells, Proc. Natl. Acad. Sci. 99 (5) (2002) 3024–3029.
[58] S. Nori, Y. Okada, A. Yasuda, O. Tsuji, Y. Takahashi, Y. Kobayashi, K. Fujiyoshi, M. Koike, Y. Uchiyama, E. Ikeda, Grafted human-induced pluripotent stem-cell–derived neurospheres promote motor functional recovery after spinal cord injury in mice, Proc. Natl. Acad. Sci. 2011 (2011) 1–6.
[59] V.M. Tysseling-Mattiace, V. Sahni, K.L. Niece, D. Birch, C. Czeisler, M.G. Fehlings, S.I. Stupp, J.A. Kessler, Self-assembling nanofibers inhibit glial scar formation and promote axon elongation after spinal cord injury, J. Neurosci. 28 (14) (2008) 3814–3823.

Please cite this article as: Z. Fan, X. Liao and Y. Tian et al., A prevascularized nerve conduit based on a stem cell sheet effectively promotes the repair of transected spinal cord injury, Acta Biomaterialia, https://doi.org/10.1016/j.actbio.2019.10.042